Organosilica Multilamellar Vesicles with Tunable Number of Layers and Sponge-Like Walls via One Surfactant Templating

Yang Zhang,[†] Meihua Yu,[†] Liang Zhou,[†] Xufeng Zhou,[†] Qingfei Zhao,[‡] Hexing Li,[‡] and Chengzhong Yu*,[†]

Department of Chemistry and Shanghai Key Laboratory of Molecular Catalysis and Innovative Materials, Fudan University, Shanghai 200433, P.R. China, and Department of Chemistry, Shanghai Normal University, Shanghai 200234, P.R. China

Received April 30, 2008. Revised Manuscript Received July 13, 2008

Organosiliceous multilamellar vesicles (MLVs) have been prepared with a high yield (>90%) and at mild conditions, through a single-templating approach by using Pluronic P85 as a structure directing agent and 1,2-bis(triethoxysilyl)ethane (BTEE) as an organosilica source. The obtained vesicles have diameters of 100−200 nm and possess sponge-like walls with the mesopore size centered at 6 nm. The number of layers can be adjusted from 7 to 1 by changing the synthesis pH value from 4.8 to 5.2. The specific surface area and pore volume of organosilica MLVs are as large as 695 m^2/g and 2.10 cm^3/g, respectively. Moreover, a transformation from the hexagonal mesostructure obtained at pH 4.2 to multilamellar (pH 4.8−5.2) and unilamellar vesicles (pH 5.5) is observed. The organosilica MLVs with controlled wall thickness, hierarchical porosity, and interconnected sponge-like walls are promising candidates for applications in nanoreactors, selective sorption, and controlled release.

Introduction

Organic vesicles can be spontaneously assembled from compounds such as lipids,[1] catanionic surfactants,[2] and block copolymers,[3,4] while inorganic vesicles are usually obtained by direct vesicle-templating[5] or utilizing synergetic self-assembly of organic molecules and inorganic precursors.[6] Recently, siliceous vesicles as well as hollow spheres with large voids have attracted much attention, because these materials possess high surface area and low density, as well as enhanced thermal stability and robustness, compared to their organic counterparts, thus showing great application potentials as chromatography matrices,[7] absorbents,[6] nanocatalysts,[8] microcapsules,[9] and controlled release/delivery carriers.[10−12]

For the applications of vesicles and hollow spheres where the host−guest surface interactions and the transport of guest molecules in and out of the voids are involved, the number of layers (or the thickness), the porous structure, and the composition of walls are crucial factors. Moreover, the fabrication of hollow morphology at a high yield and through a simple approach is an important issue. Mesoporous hollow spheres can be obtained through colloid templating,[13] emulsion templating,[10,14−16] multisurfactant templating,[17] or single crystal templating[18] approaches. These methods generally involve multistep operations, complex components, or unusual additives and hence are less economical or convenient than the single surfactant vesicle templating approach, which utilizes the phase behavior of surfactants. Through the single surfactant approach, several hierarchically porous vesicular structures have been synthesized.[19−23] For example, Seong et al. first reported the synthesis of vesicular materials

* Corresponding author. E-mail: czyu@fudan.edu.cn.
[†] Fudan University.
[‡] Shanghai Normal University.

(1) Warriner, H. E.; Idziak, S. H. J.; Slack, N. L.; Davidson, P.; Safinya, C. R. *Science* **1996**, *271*, 969.
(2) Marques, E. F.; Regev, O.; Khan, A.; da GracaMiguel, M.; Lindman, B. *J. Phys. Chem. B* **1998**, *102*, 6746.
(3) Zhang, L.; Eisenberg, A. *Science* **1995**, *268*, 1728.
(4) Discher, B. M.; Won, Y.-Y.; Ege, D. S.; Lee, J. C.-M.; Bates, F. S.; Discher, D. E.; Hammer, D. A. *Science* **1999**, *284*, 1143.
(5) Hubert, D. H. W.; Jung, M.; German, A. L. *Adv. Mater.* **2000**, *12*, 1291.
(6) Wang, H. N.; Wang, Y. H.; Zhou, X. F.; Zhou, L.; Tang, J. W.; Lei, J.; Yu, C. Z. *Adv. Funct. Mater.* **2007**, *17*, 613.
(7) Gallis, K. W.; Araujo, J. T.; Duff, K. J.; Moore, J. G.; Landry, C. C. *Adv. Mater.* **1999**, *11*, 1452.
(8) Pablo, M.; Arnal, M. C. F. S. *Angew. Chem., Int. Ed.* **2006**, *45*, 8224.
(9) Kim, J.; Lee, J.; Na, H. B.; Kim, B. C.; Youn, J. K.; Kwak, J. H.; Moon, K.; Lee, E.; Kim, J.; Park, J.; Dohnalkova, A.; Park, H. G.; Gu, M. B.; Chang, H. N.; Grate, J. W.; Hyeon, T. *Small* **2005**, *1*, 1203.
(10) Botterhuis, N. E.; Sun, Q.; Magusin, P. C. M. M.; van Santen, R. A.; Sommerdijk, N. A. J. M. *Chem. Eur. J.* **2006**, *12*, 1448.
(11) Chen, J.-F.; Ding, H.-M.; Wang, J.-X.; Shao, L. *Biomaterials* **2004**, *25*, 723.
(12) Zhu, Y.; Shi, J.; Shen, W.; Dong, X.; Feng, J.; Ruan, M.; Li, Y. *Angew. Chem., Int. Ed.* **2005**, *44*, 5083.
(13) Caruso, F.; Caruso, R. A.; Möhwald, H. *Science* **1998**, *282*, 1111.
(14) Schacht, S.; Huo, Q.; Voigt-Martin, I. G.; Stucky, G. D.; Schüth, F. *Science* **1996**, *273*, 768.
(15) Sun, Q.; Kooyman, P. J.; Grossmann, J. G.; Bomans, P. H. H.; Frederik, P. M.; Magusin, P. C. M. M.; Beelen, T. P. M.; van Santen, R. A.; Sommerdijk, N. A. J. M. *Adv. Mater.* **2003**, *15*, 1097.
(16) Wang, J.; Xiao, Q.; Zhou, H.; Sun, P.; Yuan, Z.; Li, B.; Ding, D.; Shi, A. C.; Chen, T. *Adv. Mater.* **2006**, *18*, 3284.
(17) Yeh, Y. Q.; Chen, B. C.; Lin, H. P.; Tang, C. Y. *Langmuir* **2006**, *22*, 6.
(18) Jiang, X.; Brinker, C. J. *J. Am. Chem. Soc.* **2006**, *128*, 4512.
(19) Kim, S. S.; Zhang, W.; Pinnavaia, T. J. *Science* **1998**, *282*, 1302.
(20) Tan, B.; Vyas, S. M.; Lehmler, H. J.; Knutson, B. L.; Rankin, S. E. *Adv. Funct. Mater.* **2007**, *17*, 2500.
(21) Yu, M. H.; Wang, H. N.; Zhou, X. F.; Yuan, P.; Yu, C. Z. *J. Am. Chem. Soc.* **2007**, *129*, 14576.
(22) Tan, B.; Lehmler, H.-J.; Vyas, S. M.; Knutson, B. L.; Rankin, S. E. *Adv. Mater.* **2005**, *17*, 2368.
(23) Yuan, P.; Yang, S.; Wang, H.; Yu, M.; Zhou, X.; Lu, G.; Zou, J.; Yu, C. *Langmuir* **2008**, *24*, 5038.

10.1021/cm8011815 CCC: $40.75 © 2008 American Chemical Society
Published on Web 08/30/2008

with Lα−L_3 intermediate mesostructured walls, which possess interconnected pores (∼3 nm in diameter) within multilamellar walls.[19] The former Lα is a standard lamellar phase[1] while the latter represents a 3-D sponge-like porous structure.[24] However, most of the spherical morphologies of vesicles were severely ruptured. Up to now, it is extremely difficult to finely tune the wall thickness of vesicles; the attempt to synthesize siliceous vesicles with controlled number of layers and porous wall structures by one surfactant remains unsuccessful.

The composition of silica-based vesicles can be adjusted from pure silica to organosilica. In the latter family of materials, their physicochemical properties and functions can be modulated by further introducing various organic functional groups homogeneously distributed in the inorganic matrix.[25−30] However, organosilica vesicles are difficult to synthesize and have received less attention compared to the silica counterparts.[20,30,31] Djojoputro et al. reported the synthesis of organosilica hollow spheres with mesoporous walls (<3 nm in pore diameter) in the presence of cetyltrimethylammonium bromide (CTAB) and another fluorinated surfactant (FC4) as cotemplate under basic conditions through a liquid crystal and vesicle dual templating approach.[31] The wall thickness of particles can be tuned in a certain range (∼20−100 nm). However, the morphology of the obtained materials was not uniform and varied from hexagonal to spherical shapes depending on the FC4/CTAB ratio. It is still a great challenge to synthesize organosilica vesicles at a high yield and, especially, through a simple one-surfactant templating approach.

In this paper, we report the synthesis and characterization of organosiliceous multilamellar vesicles (MLVs) with sponge-like walls via a facile one-template approach. Commercially available triblock copolymer Pluronic P85 was chosen as a structure directing agent, and 1,2-bis(triethoxysilyl)ethane was used as an organosilica precursor. By simply varying the synthesis pH from 4.8 to 5.2, the number of the layers of vesicles can be modulated from 1 to 7. A mesostructure transformation from hexagonal phase (at pH 4.2) to multilamellar and unilamellar vesicles (at pH 5.5) is observed. Our approach is carried out at mild pH, and the resultant organosilica MLVs have interconnected sponge-like walls with relatively larger pores (∼6 nm), which provides a convenient method to synthesize functional vesicular materials with versatile applications.

Experimental Section

Chemicals. Triblock poly(ethylene oxide)-*b*-poly(propylene oxide)-*b*-poly(ethylene oxide) (PEO-PPO-PEO) copolymer Pluronic P85 ($EO_{26}PO_{39}EO_{26}$) was received as a gift from BASF company. 1,2-Bis(triethoxysilyl)ethane was purchased from Aldrich. Other chemicals were purchased from the Shanghai Chemical Co. All chemicals were used as received without further purification.

Synthesis. In a typical synthesis, 1.0 g of Pluronic P85 and 0.85 g of Na_2SO_4 were dissolved in 30 mL of HAc/NaAc buffer solution ($C_t = C_{HAc} + C_{NaAc} = 0.08$ M) with selected pH and at 60 °C. Then 1.06 g of BTEE was added to the solution, and the reactants were stirred for 20 min before being kept at static condition for 2 days. The molar ratio of reagents is P85:BTEE:Na_2SO_4:H_2O = 0.073:1:2:280. All the reactants were then transferred into an autoclave and heated at 100 °C for 1 day. After cooling down to room temperature, the precipitates were filtrated, washed with deionized water three times, and then washed with 45 mL of ethanol solution with 0.5 M HCl at 60 °C twice (6 h each time) to remove the block copolymer template. The final products were obtained by drying in air. The synthesis was carried out at six different pH points 4.2, 4.6, 4.8, 5.0, 5.2, and 5.5, and the resultant organosiliceous samples were denoted O4.2, O4.6, O4.8, O5.0, O5.2, and O5.5, respectively. The yield calculated based on organosilica for each sample is >90%.

Characterization. The scanning electron microscopy (SEM) images were recorded on a JEOL 6400 electron microscope operating at 20 kV with samples coated with gold. Transmission electron microscopy (TEM) images were obtained by a JEOL 2010 electron microscope with an acceleration voltage of 200 kV. The powder of the samples for TEM measurements was suspended in ethanol, ground in a mortar, and then loaded onto copper grids with holey carbon films. Powder X-ray diffraction (XRD) patterns were recorded using a Bruker D4 Endeavor Diffractometer with Cu Kα radiation at a voltage of 40 kV and a current of 40 mA. N_2 adsorption/desorption isotherms were measured at 77 K on a Micromeritics Tristar Surface Area and Porosity Analyzer. Before measurement, samples were evacuated at 180 °C for at least 8 h. The specific surface area (S_{BET}) was calculated by the Brunauer−Emmett−Teller (BET) method. The total pore volume (V_t) was measured at a relative pressure P/P_0 higher than 0.99. The pore size distributions and the pore diameter (D) were calculated using the Barrett−Joyner−Halenda (BJH) model. In the discussion of the porosity of organosiliceous materials, another term V_m represents only the volume of mesopores corresponding to the range of the peak centered at ∼6−7 nm, which is estimated from the BJH adsorption cumulative pore volume data. Solid-state cross-polarization magic-angle spinning (CP-MAS) ^{13}C NMR spectrum and ^{29}Si NMR spectrum were recorded with a Bruker DSX 300. The contact time for ^{13}C and ^{29}Si NMR is 1 and 5 ms, and recycling delays for ^{13}C and ^{29}Si are 2 and 3 s, respectively.

Results and Discussion

The SEM images of samples O4.8, O5.0, and O5.2 are illustrated in Figure 1a,b,c, respectively. All three samples show a spherical morphology with diameters of 100−200 nm. Several particles are broken under SEM observations, indicating that they are hollow spheres. It is noted that with increasing pH (from O4.8 to O5.2), more broken spheres with small holes are observed, suggesting that the mechanical strength of the shell is decreased. The mesostructures of samples O4.8, O5.0, and O5.2 are shown in the TEM images (Figure 1d−i). It is clearly seen that O4.8, O5.0, and O5.2 are all vesicles with core−shell structures. However, the shell

(24) McGrath, K. M.; Dabbs, D. M.; Yao, N.; Aksay, I. A.; Gruner, S. M. *Science* **1997**, *277*, 552.
(25) Asefa, T.; MacLachlan, M. J.; Coombs, N.; Ozin, G. A. *Nature* **1999**, *402*, 867.
(26) Inagaki, S.; Guan, S.; Fukushima, Y.; Ohsuna, T.; Terasaki, O. *J. Am. Chem. Soc.* **1999**, *121*, 9611.
(27) Hatton, B.; Landskron, K.; Whitnall, W.; Perovic, D.; Ozin, G. A. *Acc. Chem. Res.* **2005**, *38*, 305.
(28) Shea, K. J.; Loy, D. A. *Acc. Chem. Res.* **2001**, *34*, 707.
(29) Morell, J.; Wolter, G.; Froba, M. *Chem. Mater.* **2005**, *17*, 804.
(30) Lu, Y.; Fan, H.; Doke, N.; Loy, D. A.; Assink, R. A.; LaVan, D. A.; Brinker, C. J. *J. Am. Chem. Soc.* **2000**, *122*, 5258.
(31) Djojoputro, H.; Zhou, X. F.; Yu, C. Z.; Lu, G. Q. *J. Am. Chem. Soc.* **2006**, *128*, 6320.

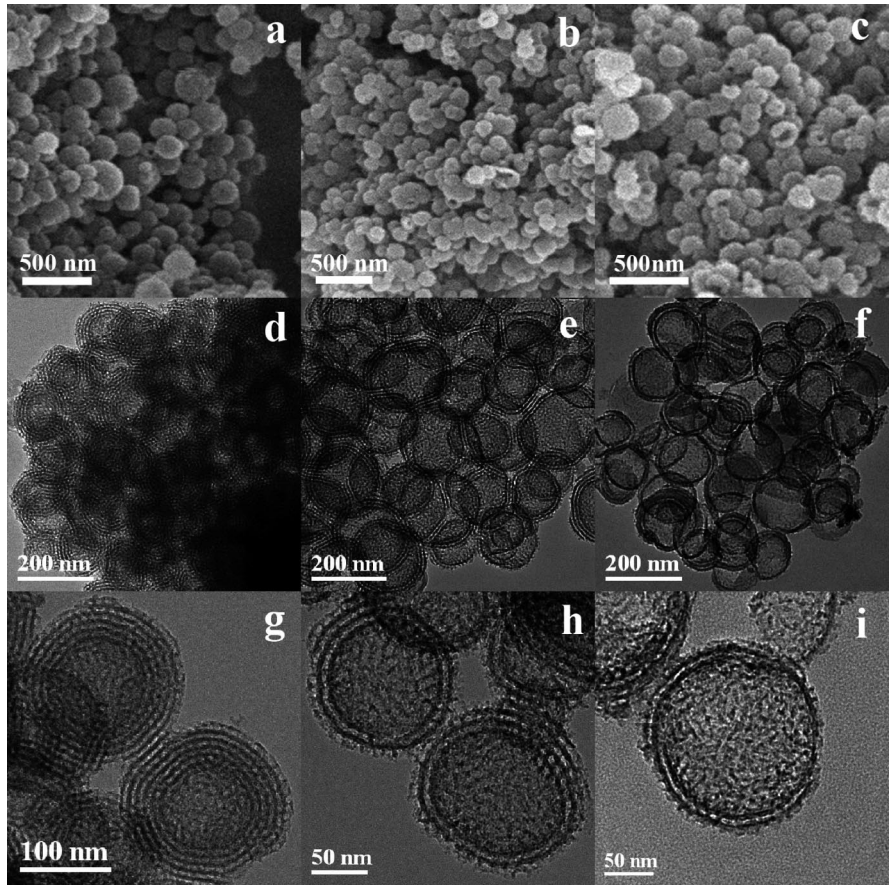

Figure 1. SEM (a, b, c), TEM (d, e, f), and high magnification TEM images (g, h, i) of organosiliceous vesicles O4.8, O5.0, and O5.2, respectively.

thickness is different in three samples. The number of layers is estimated to be 5−7, 3−4, and 1−2 for O4.8, O5.0, and O5.2, respectively. The variation in layer numbers well explains the difference in the mechanical strength among the three organosilica samples.

It is interesting to carefully examine the wall structure of organosiliceous MLVs. From high magnification TEM images (Figure 1g−i), it is seen that the lamellae of vesicles are bridged by randomly distributed tubules. This feature is most distinct for O5.2 (Figure 1i) with the smallest number of layers. For three samples, the randomly distributed pores are also observed at the rim of spheres between two adjacent layers. Some mesopores that penetrate the layers can be observed in high magnification TEM images (Supporting Information, Figure S1), suggesting the existence of interconnected nanopores. The thickness of each layer is estimated to be 4−5 nm, and the diameter of tubular mesopores is ∼6 nm. Because the layers are interconnected by tubules, these spheres can to some extent withstand distortions and maintain a relatively integral vesicular morphology. This mesostructure is consistent with former reported Lα-L_3 intermediate phase,[19] and the 3-D interconnected wall frameworks and voids with larger pore sizes compared to previous reports[19,31] may be important for future applications of organosilica MLVs.

The reaction pH is a crucial factor that influences the vesicular structure. When pH is raised to 5.5, the SEM image of sample O5.5 shows that most of the hollow spheres are broken or have an oblate morphology; some curved lamellae are also observed (Figure 2a). The TEM observation of O5.5 is in accordance with the SEM results. As can be seen from Figure 2b, generally broken unilamellar vesicles (ULVs) exist in O5.5. In addition, compared with samples prepared in the pH range of 4.8−5.2, relatively smooth surfaces with rather few mesopores are observed in O5.5. While the reaction pH is lowered to 4.2, the SEM image displays only solid particles with irregular sizes and shapes in sample O4.2 (Figure 2c). The TEM image shows that the solid particles of sample O4.2 have ordered hexagonal mesostructure (Figure 2d). To investigate the transformation from hexagonal mesostructure to MLVs, sample O4.6 was synthesized at pH 4.6. The morphology of O4.6 is heterogeneous, and only a few spherical particles are observed (Figure 2e). Under TEM observations (Figure 2f), vesicles possessing both more than 10 layers and local hexagonal mesopore arrays (marked by rectangles) are occasionally observed. The pH of 4.6 is thus considered as a transition point from a hexagonal phase to MLVs. The above results reveal that to obtain the vesicular morphology of organosiliceous materials with a high yield, the reaction pH should be carefully adjusted in the range of 4.8−5.2 in our approach.

To further investigate the mesostructure of organosiliceous materials, XRD patterns of six samples were studied (Figure 3). No diffraction peak is observed for O5.5, in accordance with the structure revealed by TEM observations (Figure 2b). For O5.2, O5.0, and O4.8, generally one broad diffraction peak is observed, indicating a disordered mesostructure consistent with the sponge-like wall structure shown in Figure

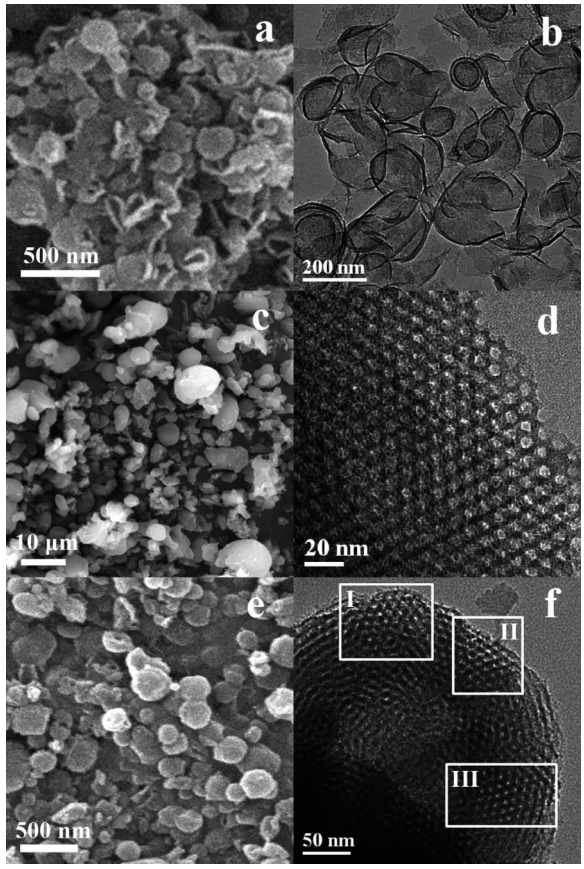

Figure 2. SEM (a, c, e) and TEM (b, d, f) images of organosiliceous samples O5.5, O4.2, and O4.6, respectively.

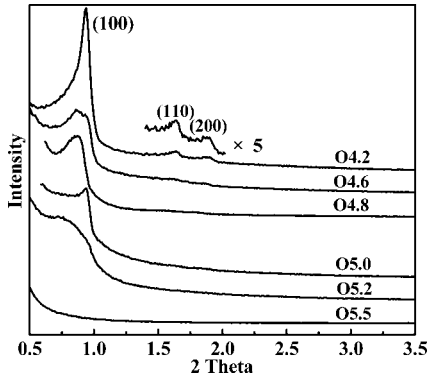

Figure 3. XRD patterns of samples O4.2, O4.6, O4.8, O5.0, O5.2, and O5.5.

1g−i. In contrast, three diffraction peaks can be observed in the XRD pattern of O4.2, which can be indexed to the (100), (110), and (200) diffractions of a 2-D hexagonal mesostructure. Compared to that of O4.2, the XRD pattern of O4.6 shows a broader first diffraction peak, and the diffractions at higher angles are also discernible but with very low intensity, consistent with the TEM observation of O4.6 (Figure 2f). The XRD results reveal that ordered hexagonal mesostructures of organosiliceous materials can be synthesized at pH $\leq$ 4.2, and a phase transition from multilamellar to hexagonal phase occurs at the pH of 4.6.

The N_2 sorption analysis was performed for all the organosilica samples obtained in our study. For the isotherms of samples synthesized at increasing pH (from O4.2 to O5.5), the volume adsorbed at the capillary condensation step occurring at P/P_0 of 0.6−0.7 gradually decreases, while the volume adsorbed at another step occurring at higher P/P_0 of $\sim$ 0.9 becomes more remarkable (Figure 4a). The trend of varying pore volumes can also be seen from the pore size distribution curves calculated from the adsorption branch (Figure 4b). The peaks centered at 4−9 nm corresponding to the condensation step occurring at P/P_0 of 0.6−0.7 decrease continuously when the reaction pH is increased. The small hysteresis loops of all the samples suggest that the pore throats (or so-called "windows") are adequately large, showing little difference in the mesopores in diameter. The relatively large pore vesicles with 3-D interconnected walls without marked throats are beneficial for mass transfer in future applications.

The physicochemical and structural properties of the organosiliceous samples are summarized in Table 1. While the reaction pH is increased, the surface area of organosilica materials generally decreases, in accordance with the transition from a highly porous structure (O4.2) to a relatively smooth lamellar structure (O5.5). The gradual decrease in the mesopore volume (V_m, in the range of 4−9 nm) as the reaction pH increases is also consistent with the structures of organosiliceous samples. It is not surprising that O4.2 and O5.5 have the largest (0.62 cm^3/g) and smallest (0.07 cm^3/g) mesopore volumes, respectively. For the organosiliceous MLVs, the mesopore volume decreases in the order of O4.8 > O5.0 > O5.2, reflecting the same sequence of the number of layers in three MLVs with sponge-like walls of different wall thickness. It is also noted that the three MLVs have relatively large pore sizes (6.2−6.5 nm) and high pore volumes (0.94−2.10 cm^3/g) compared to other organosiliceous vesicles.[19,31] Sample O5.0 with the intermediate number of layers among three MLVs has the largest pore volume of 2.10 cm^3/g. For O4.8, the increase in the wall thickness may decrease the void volume in terms of unit mass (0.94 cm^3/g). While for O5.2 with smaller number of layers, the intact vesicular morphology may be partly damaged for the decrease in mechanical strength, leading to a decreased pore volume of 1.55 cm^3/g. The organosiliceous MLVs with sponge-like walls, tunable number of layers, high pore volumes, and large pore sizes possess great potential in their future applications such as controlled release and so forth.

To confirm the integrity of organic moieties in framework, ^{29}Si and ^{13}C NMR measurements have been conducted. Considering the similarity of these samples synthesized in a small pH range, the information for only one sample O5.0 is presented. In the solid-state ^{29}Si NMR spectrum (Figure 5a), only T^1, T^2, and T^3 peaks ($C-C-Si-(OSi)_1(OH)_2$, $C-C-Si-(OSi)_2(OH)_1$, and $C-C-Si-(OSi)_3$, respectively) with increasing intensities at −46, −57, and −63 ppm are observed, and no obvious Q^1-Q^4 peaks ($Si-(OSi)_x(OH)_{4-x}$, $x = 1-4$) at lower ppm appear,[25] indicative of the absence of Si−C bond cleavage in the mild reaction conditions. In the ^{13}C NMR spectrum (Figure 5b), the peak at 4.9 ppm is attributed to the bridging ethylene carbon of the $-SiCH_2CH_2Si-$ moieties. The tiny peaks at 15.7 and 70.7 ppm are associated with the signals of methyl and methylene carbon atoms of

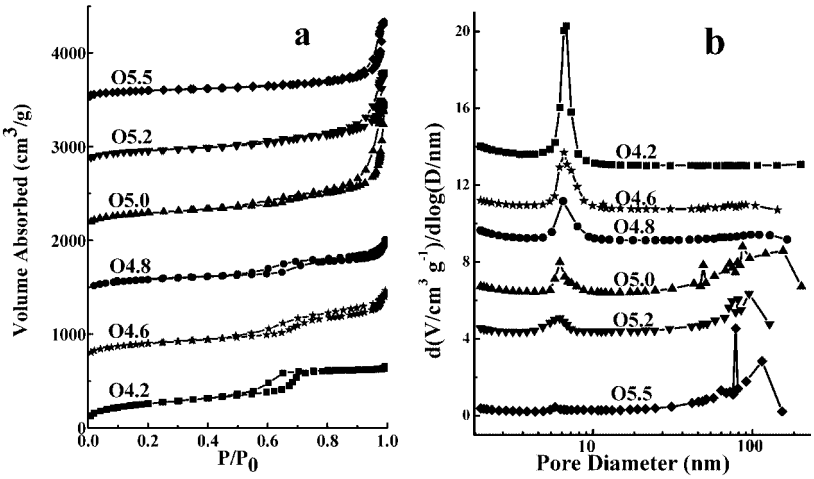

Figure 4. Nitrogen sorption isotherms (a) and pore size distribution curves calculated from the adsorption branches (b) for samples O4.2−O5.5. The *Y*-axis values in (a) are shifted upward by 700, 1400, 2100, 2800, and 3500 cm^3/g for O4.6−O5.5, respectively. The *Y*-axis values in (b) are shifted upward by 4, 6, 9, 10.5, and 13 cm^3/g for O5.2, O5.0, O4.8, O4.6, and O4.2, respectively.

Table 1. Physicochemical Properties of Organosiliceous Samples

sample	structure[a]	N_l[b]	S_{BET} (m^2/g)	V_m (cm^3/g)	V_t (cm^3/g)	D (nm)
O4.2	Hex		935	0.62	1.01	6.8
O4.6	MLV + Hex	>10	721	0.43	1.18	6.6
O4.8	MLV	5−7	654	0.31	0.94	6.5
O5.0	MLV	3−4	695	0.25	2.10	6.2
O5.2	MLV	1−2	575	0.19	1.55	6.2
O5.5	ULV	1	355	0.07	1.29	5.8

[a] For the structure of materials, "Hex" represents "hexagonal". [b] N_l: the number of layers.

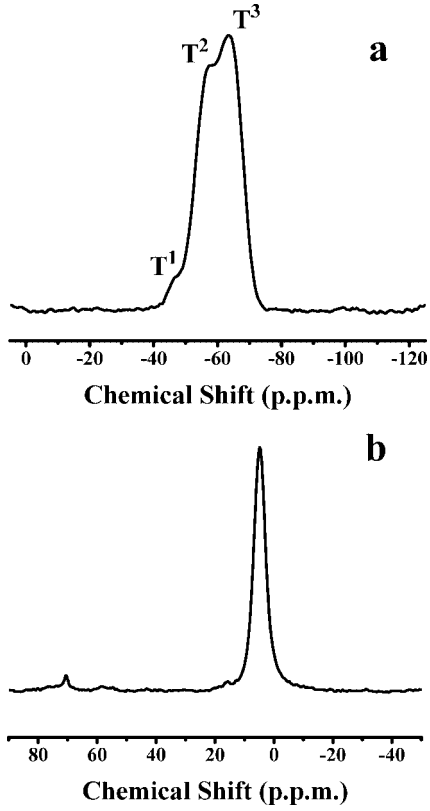

Figure 5. Solid-state ^{29}Si NMR spectrum (a) and ^{13}C NMR spectrum (b) of sample O5.0.

surface ethoxy groups ($Si\text{-}OCH_2CH_3$) grafted during the process of ethanol extraction, respectively.[32] No other peak can be found in the ^{13}C NMR spectrum of the organosilica sample, demonstrating that the Si−C bond is well maintained in our synthesis. The above result also implies that the ethanol extraction process can effectively remove most surfactant molecules from the as-synthesized organosilica samples.

In our approach, the reaction pH plays double roles in inducing the structural transition and tuning the number of layers of MLVs. First, it is well-known that by increasing the reaction pH, the deprotonation of the EO moieties will decrease their hydrophilicity, thus leading to the structural transition from an ordered hexagonal structure to lamellar structures[33] with sponge-like walls.[19] Second, the formation of MLVs with desired number of layers depends on the competition between bending energy and layer-to-layer interactions.[34] The bending energy will increase when MLVs with a larger number of layers are formed. The formation of organized organic−inorganic composites is a cooperative self-assembly process;[35] thus, the variation in inorganic species is also important to influence the final structure. It is well-known that the hydrolysis rate increases when the pH is lowered (at pH < 7).[36] In our experiments, it was observed that the oil phase (BTEE) disappeared first in the most acidic solution. Moreover, the precipitation time for O4.8, O5.0, and O5.2 was measured to be 6, 8, and 11 h, respectively, indicative of a higher hydrolysis and condensation rate at lower pH. Therefore, it is suggested that at a given time the concentration of hydrolyzed organosilica species with silanols is larger in a more acidic condition. The enhanced cross-linking of lamellae due to the condensation of silanols with increased concentrations will compensate for the increase in bending energy; thus, the formation of MLVs with more layers is favored (e.g., in sample O4.8).

(32) Liang, Y.; Hanzlik, M.; Anwander, R. *J. Mater. Chem.* **2005**, *15*, 3919.
(33) Huo, Q.; Margolese, D. I.; Stucky, G. D. *Chem. Mater.* **1996**, *8*, 1147.
(34) Jung, H. T.; Coldren, B.; Zasadzinski, J. A.; Iampietro, D. J.; Kaler, E. W. *Proc. Natl. Acad. Sci.* **2001**, *98*, 1353.
(35) Monnier, A.; Schuth, F.; Huo, Q.; Kumar, D.; Margolese, D.; Maxwell, R. S.; Stucky, G. D.; Krishnamurty, M.; Petroff, P.; Firouzi, A.; Janicke, M.; Chmelka, B. F. *Science* **1993**, *261*, 1299.
(36) Brinker, C. J.; Scherer, G. W. *Sol-Gel Science: The Physics and Chemistry of Sol-Gel Processing*; Academic Press: New York, 1990.

Conclusion

In conclusion, organosiliceous vesicles have been successfully synthesized via a facile single-template approach with a high yield and at mild conditions. Moreover, these vesicles have a tunable number of layers, sponge-like organosilica walls, and hierarchical porosity. It is expected that this approach can be applicable to synthesize novel organosiliceous MLVs with other organic groups and new functions, which are promising candidates for applications in nanoreactors, selective ad/desorption, and controlled release.

Acknowledgment. We thank the State Key Research Program (2004CB217804, 2006CB932302), Shanghai Science Committee (06JC14011), the Ministry of Education of China (20060246010), Shanghai-Unilever Research and Development Fund (05SU07098), SLADP (B108), and NCET for their financial support.

Supporting Information Available: TEM images of O4.8 and O5.0 (PDF). This material is available free of charge via the Internet at http://pubs.acs.org.

CM8011815